Nuclear Translocation of the Tumor Marker Pyruvate Kinase M2 Induces Programmed Cell Death

Attila Steták,[1,2] Réka Veress,[2] Judit Ovádi,[4] Péter Csermely,[3] György Kéri,[2] and Axel Ullrich[1]

[1]Department of Molecular Biology, Max-Planck-Institute for Biochemistry, Martinsried, Germany; [2]Peptide Biochemistry Research Group of Hungarian Academy of Sciences; [3]Department of Medical Chemistry, Semmelweis University; and [4]Institute of Enzymology, Biological Research Center, Hungarian Academy of Sciences, Budapest, Hungary

Abstract

Cancer cells often fail to respond to stimuli that normally activate their intrinsic apoptotic machinery. Moreover, they are able to adapt to hypoxia by changing their glycolytic rate. Pyruvate kinase (PK) is a rate-limiting enzyme in glycolysis that is converted to a less active dimer form of PKM2 isoenzyme during oncogenesis. Here, we show that both somatostatin and the structural analogue TT-232 interact with the PKM subtype. We further show that the PKM2 is translocated to the nucleus in response to TT-232 and different apoptotic agents. Nuclear translocation of PKM2 is sufficient to induce cell death that is caspase independent, isoform specific, and independent of its enzymatic activity. These results show that the tumor marker PKM2 plays a general role in caspase-independent cell death of tumor cells and thereby defines this glycolytic enzyme as a novel target for cancer therapy development. [Cancer Res 2007;67(4):1602–8]

Introduction

Somatostatin is a neuropeptide hormone that was first described in 1973. The major actions of the peptide include the inhibition of hormone secretion from the pituitary, most notably that of growth hormone (1), the pancreas, and other endocrine tissues, and the inhibition of exocrine secretion in various organs. Moreover, somatostatin has antiproliferative activity and is a widely distributed neurotransmitter in the brain and the peripheral nervous system (2). Somatostatin exerts its activity via six different seven-pass transmembrane receptors (SSTR1-5). On binding the ligand, the activated receptors are able to induce diverse signaling cascades that are defined by the cell type and receptor form (3).

Because of the short half-life of natural somatostatin, much effort has been undertaken to develop somatostatin analogues with increased stability, such as octreotide, lanreotide, and vapreotide, which are used in the treatment of certain cancers. However, because of the diverse functions of somatostatin, it would be desirable to develop derivatives with more restricted physiologic actions and preserved antitumor activity.

TT-232 is a structural somatostatin analogue with a cyclopentaring structure: D-Phe-Cys-Tyr-D-Thr-Lys-Cys-Thr-NH_2. Unlike somatostatin or conventional somatostatin analogues, TT-232 does not inhibit growth hormone release or gastrin secretion *in vivo* (4) but it exerts a strong antiproliferative effect and selectively induces caspase- and Bcl-2–independent cell death in a large variety of tumor cells both *in vitro* and *in vivo* (4). We have shown previously that TT-232 acts trough seven-pass transmembrane somatostatin receptors to induce G_1 cell cycle arrest (5). This antiproliferative effect is mediated by the activation of a signaling cascade that transiently increases extracellular signal-regulated kinase (Erk)/mitogen-activated protein kinase activity and leads to the transcriptional activation and accumulation of $p21^{CIP1}$ cyclin-dependent kinase inhibitor protein (5, 6). However, we found that inhibition of this signaling cascade is not sufficient to block TT-232–induced cell death. According to morphologic criteria (7) and DNA ladder formation (8), this cell death could be classified as apoptosis. Furthermore, the apoptotic activity of TT-232 requires endocytosis of the drug (4, 7, 8–10).[5] These data suggest that TT-232 acts in a dual way: through a somatostatin receptor-mediated signaling cascade that causes cell cycle arrest as well as via a thus far uncharacterized mechanism that induces apoptosis in tumor cells.

Pyruvate kinase (PK; ATP: pyruvate 2-*O*-phosphotransferase) is a rate-controlling enzyme of the glycolytic cascade that catalyses the formation of pyruvate and ATP from phosphoenol pyruvate and ADP (11–13). In mammals, PK exists in the form of four isozymes designated M1, M2, L, and R, which are differentially expressed in different cell types (11). Besides its well-known role in glycolysis, PK has been reported to be the cytosolic receptor for thyroid hormone (14) to influence microtubule stability (15) and to interact with phospholipids (15). Alternatively spliced products of the M isoform gene yield the M1 and M2 isotypes. The difference between these two isoforms lies in one exon encoding 51 amino acid residues, of which 21 are distinct (16). The M2 type (PKM2) is considered to be expressed predominantly in the fetus, in neoplastic tissues, and in undifferentiated or proliferating cells but is also found in some adult tissues as a tetrameric form (16, 17). During tumorigenesis, the tissue characteristic PK isoform is replaced by PKM2 that is present predominantly as a dimer (18) and seems to represent a tumor-specific form (19, 20). The dissociation of the tetrameric to the dimeric form can be induced by oncoproteins (21). Furthermore, only the tetrameric form of PKM2 is associated within the glycolytic enzyme complex, whereas the dimeric form is not.

Materials and Methods

Reagents, antibodies, and plasmid constructs. BS^3 homobifunctional cross-linker was applied as described previously (22). Antibodies purchased were mouse monoclonal histone H1 (clone AE-4; Santa Cruz Biotechnology, Santa Cruz, CA), rabbit polyclonal Erk-2 (Santa Cruz Biotechnology), mouse

[5] T. Vántus, unpublished data.

Note: Current address for Attila Steták: Institute of Zoology, University of Zürich, Winterthurerstrasse 190, 8057 Zürich, Switzerland.

Requests for reprints: Attila Steták, Institute of Zoology, University of Zürich, Winterthurerstrasse 190, 8057 Zürich, Switzerland. Phone: 41-43-635-6626; E-mail: stetak@zool.unizh.ch and Axel Ullrich, Department of Molecular Biology, Max-Planck-Institute for Biochemistry, Am Klopferspitz 18A, Martinsried, Germany. Phone: 49-89-85782512; Fax: 49-89-85782454; E-mail: ullrich@biochem.mpg.de.

doi:10.1158/0008-5472.CAN-06-2870

monoclonal green fluorescent protein (GFP; Clontech, Palo Alto, CA), mouse monoclonal tubulin (Sigma, St. Louis, MO), and rabbit polyclonal cleaved caspase-3 (Asp^{175}) antibody (Cell Signaling Technology, Inc. Boston MA). PKM2-specific polyclonal antibody was a kind gift of Dr. G. Staal (University Hospital Utrecht, Utrecht, the Netherlands) (23). Respective secondary antibodies were obtained form Bio-Rad (Hercules, CA) and Dianova (Hamburg, Germany). For immunoblot detection, the enhanced chemiluminescence system (Amersham, Uppsala, Sweden) was used. zVAD-(OMe)-FMK pan-caspase inhibitor was from Calbiochem (San Diego, CA). All other reagents were from Sigma. PKM2 was cloned from A431 cell cDNA library using PCR. The cloned gene was confirmed by DNA sequencing and cloned in-frame into either pEGFP-C1 or pEYFP-NLS (Clontech).

Terminal deoxynucleotidyl transferase–mediated dUTP nick end labeling assay. Staining was done with a terminal deoxynucleotidyl transferase–mediated dUTP nick end labeling (TUNEL) apoptosis detection kit (Upstate, Lake Placid, NY) as suggested by manufacturer. Briefly, treated cells were fixed with 4% paraformaldehyde and permeabilized with 0.05% Tween 20, and TdT end labeling with biotin-dUTP was done for 60 min at room temperature. Following washing and blocking, streptavidin-TRITC was applied for 30 min. Cells were washed, counterstained with Hoechst 33342 dye, and covered with Vectashield (Vector Laboratories, Burlingame, CA).

Fast protein liquid chromatography purification. Gel filtration was done in a Superdex 200 HR 12/60 column; the MonoQ purification was at pH 7.8 with a 0 to 0.5 mol/L NaCl gradient and the hydroxyapatite isolation with 0 to 1.0 mol/L Na-phosphate linear gradient. Each fraction was analyzed for the presence of TT-232 binding protein, and the positive fractions were pooled and subjected for further purification.

Cell culture and transfection. Cos-7 cells (American Type Culture Collection, Manassas, VA) were cultured in DMEM supplemented with 10% FCS. Cos-7 cells were transiently transfected using LipofectAMINE Plus (Life Technologies, Rockville, MD). Transfections were made in six-well dishes and in 1 mL serum-free medium containing 10 μL LipofectAMINE and 0.3 to 2 μg total plasmid DNA per well. The transfection mixtures were changed after 4 h to 10% FCS-containing medium, and cells were cultured for further 48 h. Stable cell lines were established with G418 selection. Cell clones were isolated and tested for PKM2 expression using Western blot.

Cell lysis and immunoblotting. Ninety percent confluent cells were starved for 24 h, treated as indicated, washed once with PBS, and lysed for 5 min on ice in buffer containing 50 mmol/L HEPES (pH 7.5), 150 mmol/L NaCl, 1% Triton X-100, 1 mmol/L EDTA, 10% glycerol, 10 mmol/L sodium pyrophosphate, 2 mmol/L sodium vanadate, 10 mmol/L sodium fluoride, 1 mmol/L phenylmethylsulfonyl fluoride, 10 μg/mL aprotinin, and 2 μg/mL leupeptin. Lysates were precleaned by centrifugation at 13,000 rpm (10,000 × *g*) for 5 min at 4°C. Samples were boiled in SDS sample buffer, subjected to gel electrophoresis, and transferred to nitrocellulose in a semidry blotting apparatus with 0.8 mA/cm^2 current for 2 h.

Nuclear protein extraction. Cos-7 cells were separated into cytosol and nucleus using an iso-osmotic buffer containing nonionic detergent. Cells (10^6) were treated as indicated, rinsed twice with ice-cold PBS, and

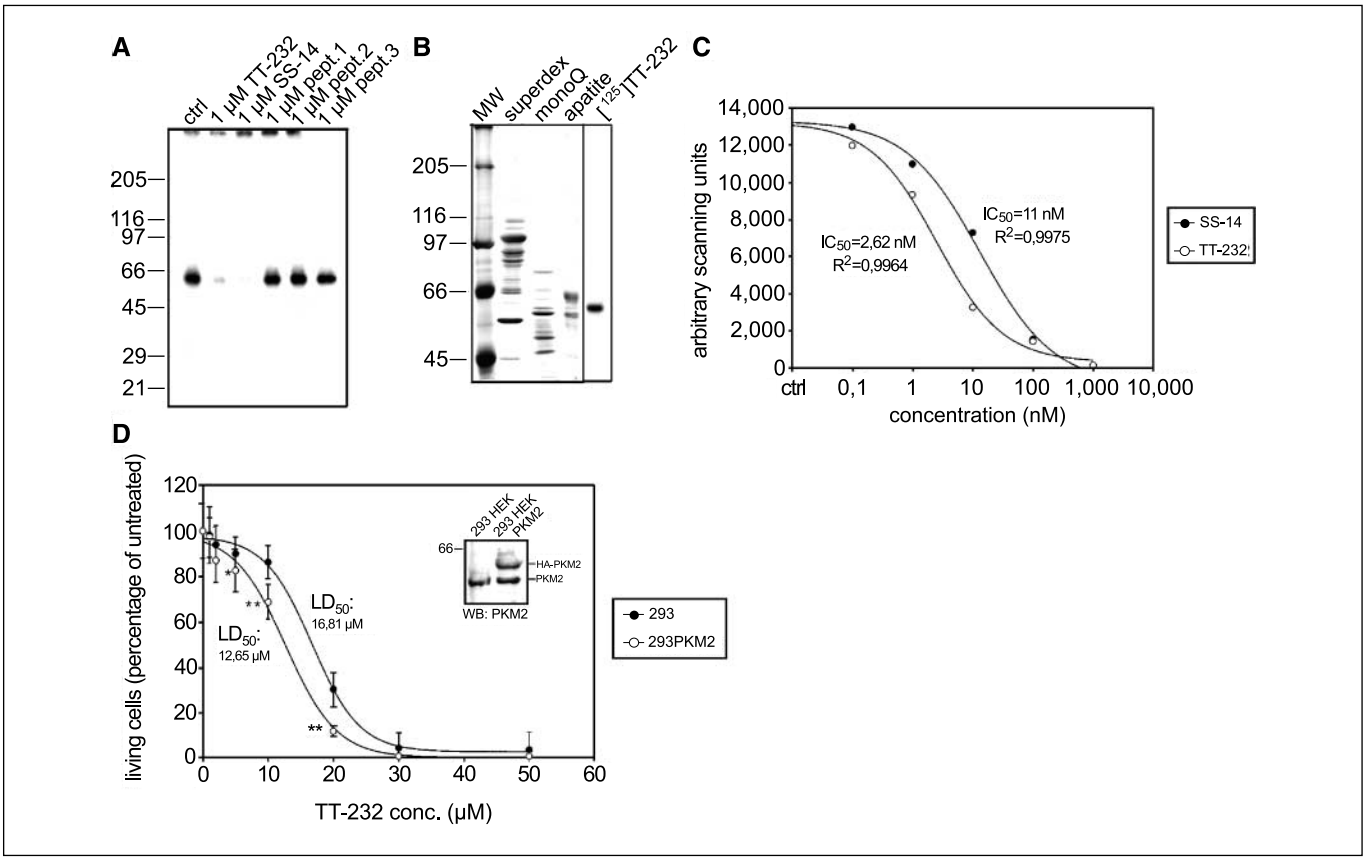

Figure 1. Identification of the TT-232 interacting protein. *A,* A431 cell lysates were mixed together with [^{125}I]TT-232 and water (*ctrl*), 1 μmol/L TT-232, somatostatin (*SS-14*), or different structurally unrelated peptides [PTPα αα 480–491 (*pept.1*), Flk-1 αα 1–11 (*pept.2*), and PTPκ αα 125–135 (*pept.3*)], cross-linked with BS^3 homobifunctional cross-linker as described (28), and subjected to gradient SDS-PAGE. *B,* the TT-232 interacting protein was sequentially purified from A431 cell lysates by FPLC. After three rounds of purification, the receptor-containing fraction was separated by SDS-PAGE and the corresponding band was isolated and identified by tryptic fragment mass spectroscopy. *C,* 2 μg of isolated PKM1 protein was incubated in the presence of 10 mmol/L $MgCl_2$ with [^{125}I]Tyr^{14}-somatostatin together with an increasing amount of unlabeled TT-232 or somatostatin (*SS-14*) Bound peptides were cross-linked to PKM1 with BS^3 cross-linker, and samples were subjected to SDS-PAGE and quantified with phosphoimager. *D,* HEK293 (*293*) or HEK293 cells stably overexpressing PKM2 (*293PKM2*) were treated with an increasing amount of TT-232 for 24 h, and cell viability was measured with the MTT assay. LD_{50} values are the average of three independent experiments. *, $P > 0.05$; **, $P > 0.01$; *bars*, SD. The amount of PKM2 was tested using Western blot (*inset*).

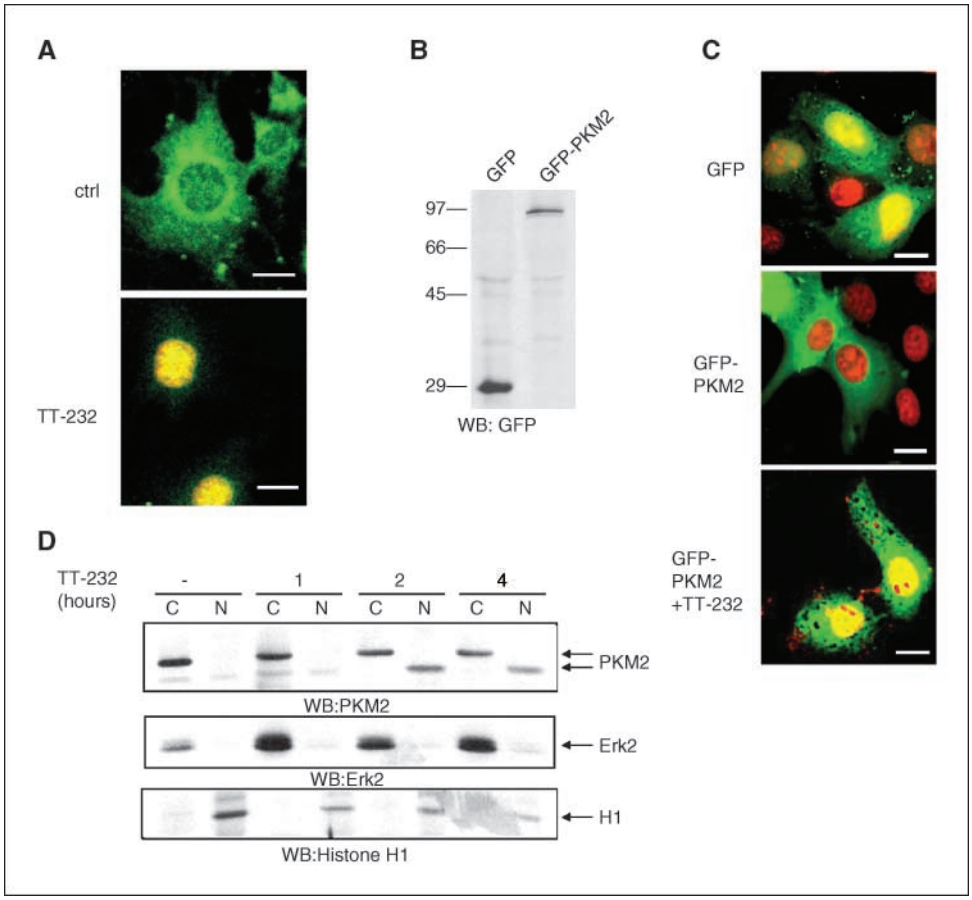

Figure 2. TT-232 stimulates the nuclear translocation of PKM2. *A,* Cos-7 cells were mock treated (*ctrl*) or treated with 50 μmol/L TT-232 for 4 h (*TT-232*), subsequently fixed, and stained with a polyclonal PKM2 antibody (*green*) as well as with Hoechst 33258 (*red*). *Scalebar*, 50 μm. *B,* expression of GFP or GFP-PKM2 was analyzed by Western blotting (*WB*) of transfected Cos-7 cell extracts. *C,* Cos-7 cells transfected with pEGFP (*GFP*) or with pEGFP-PKM2 were mock treated (*GFP-PKM2*) or treated with 50 μmol/L TT-232 for 4 h (*GFP-PKM2+TT-232*). Glutaraldehyde-fixed cells were analyzed for GFP fluorescence and stained with Hoechst 33258 to visualize nuclei (*red*). *Scalebar*, 50 μm. *D,* Cos-7 cells were untreated or treated with 50 μmol/L TT-232 for different times. Cells were separated into cytosolic (*C*) or nuclear (*N*) fractions, loaded in triplicate to a SDS gel, and blotted with PKM2 (*top*), Erk-2 (*middle*), or histone H1 (*bottom*).

scrapped and collected by centrifugation for 5 min at 500 × *g*. Pellet was vortexed for 15 sec in 200 μL NP40 lysis buffer [10 mmol/L Tris-HCl (pH 7.4), 10 mmol/L NaCl, 3 mmol/L $MgCl_2$, 0.5% NP40]. Cells were incubated for 5 min on ice and analyzed in phase-contrast microscope for complete lysis of the cytoplasm. Nuclei were centrifuged for 5 min at 500 × *g*, and SDS sample buffer was added separately to both supernatant and pellet, subjected to gel electrophoresis, and transferred to nitrocellulose in a semidry blotting apparatus with 0.8 mA/cm^2 current for 2 h.

Hoechst staining for detection of apoptosis. Subconfluent Cos-7 cells were grown on LabTek chamber slides and transfected as described. Cells were fixed with 1% glutaraldehyde in PBS for 15 min and washed twice with PBS and once with PBS supplemented with 0.25% Triton X-100.

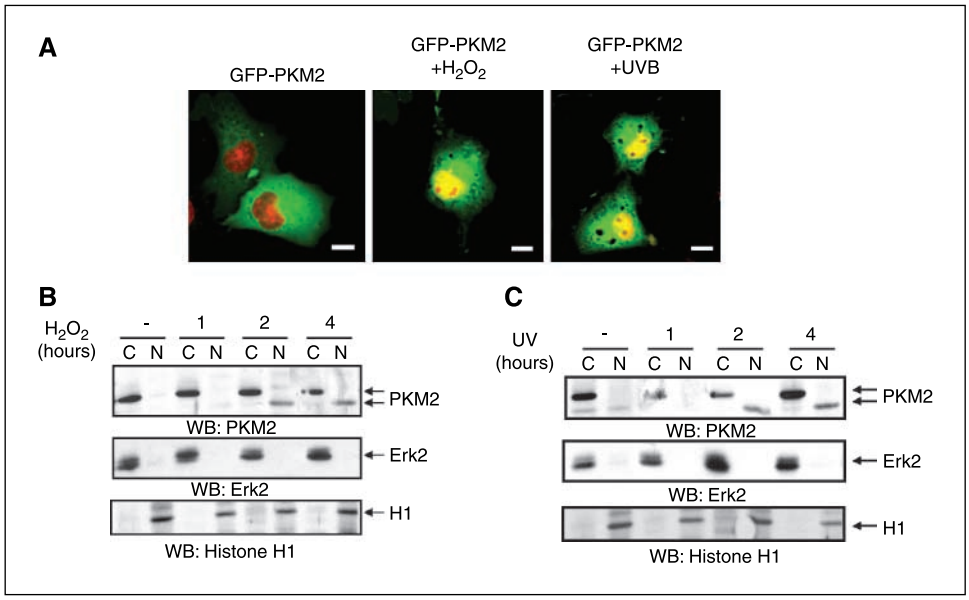

Figure 3. PKM2 translocates to the nucleus on H_2O_2 or UV treatment. *A,* Cos-7 cells were transfected with pEGFP-PKM2, untreated (*GFP-PKM2*), treated with 100 μmol/L H_2O_2 or 120 mJ/cm^2 UV (*UVB*), and incubated further for 4 h. Glutaraldehyde-fixed cells were stained with Hoechst 33258 to visualize nuclei (*red*). *Scalebar*, 50 μm. *B* and *C,* Cos-7 cells were untreated, treated with 100 μmol/L H_2O_2. (*B*) or 120 mJ/cm^2 UV (*C*), and incubated for different times. Cells were separated into cytosolic (*C*) or nuclear (*N*) fractions, loaded in triplicate, and blotted with PKM2 (*top*), Erk-2 (*middle*), or histone H1 (*bottom*).

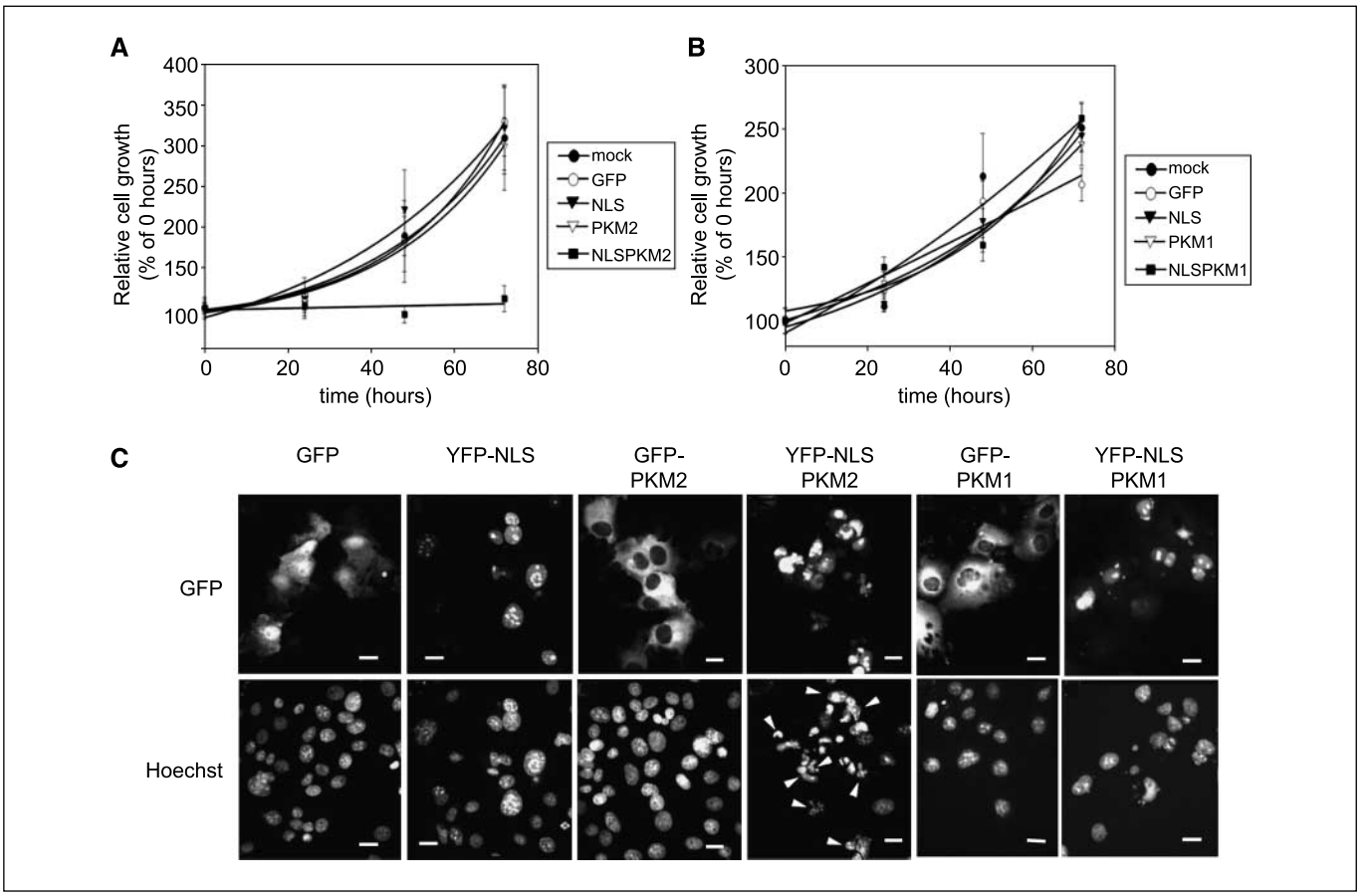

Figure 4. Nuclear targeting of PKM2 induces cell death. *A* and *B,* Cos-7 cells were transfected with empty vectors (*mock*), EYFP fused to the SV40 large T-antigen NLS, pEGFP-PKM2 (*PKM2*), or pEYFP-NLS-PKM2 (*NLS-PKM2*; *A*) or with pEGFP-PKM1 (*PKM1*) or pEYFP-NLS-PKM1 (*NLS-PKM1*; *B*). Cells were trypsinized, plated into 96-well plates, and incubated for 24, 48, and 72 h in FCS-containing medium, and cell viability was measured with the MTT assay. Before trypsinization, cells were let to adhere for 10 h and measured and this was considered as zero time point ($n = 12$ of three independent experiments). *C,* Cos-7 cells were transfected with pEGFP (*GFP*), pEYFP-NLS (*YFP-NLS*), pEGFP-PKM2 (*GFP-PKM2*), pEYFP-NLS-PKM2 (*YFP-NLS-PKM2*), pEGFP-PKM1 (*GFP-PKM1*), or pEYFP-NLS-PKM1 (*YFP-NLS-PKM1*) and incubated for 48 h in FCS-containing medium. Cells were fixed and analyzed under fluorescent microscope for GFP (*top*) and for nuclear staining (*bottom*). Highly fluorescent, condensed, fragmented nuclei were considered as being apoptotic (*arrowheads*). *Scalebar*, 50 μm.

Permeabilized cells were stained with Hoechst 33342 dye. After discarding the excess of the dye, cells were washed and covered with Vectashield. Highly fluorescent, condensed, fragmented nuclei that showed patches of compact chromatin were considered as being apoptotic.

Results

Identification of an alternate somatostatin receptor protein. To obtain better mechanistic understanding of the apoptotic activity of TT-232, we searched for potential interacting proteins by incubating [^{125}I]TT-232 with A431 cell lysates in the presence of BS^3, an NH_2-reactive, homobifunctional noncleavable cross-linker. A 60-kDa protein was detected, which interacted specifically with both TT-232 and somatostatin (Fig. 1*A*). This protein was sequentially purified by fast protein liquid chromatography (FPLC), isolated from SDS-PAGE (Fig. 1*B*), and identified by tryptic fragment tandem mass spectroscopy. The isolated protein represented the glycolytic enzyme PKM isoform. Next, using [^{125}I]Tyr^{14}-somatostatin, we confirmed the interaction in a competition assay between somatostatin, TT-232, and rabbit muscle PKM1 *in vitro*. Both somatostatin and TT-232 were found to bind with high affinity to isolated PKM1 (Fig. 1*C*) as well as to bacterially expressed PKM2 (data not shown). We investigated the role of PKM2 in TT-232–induced cell death and observed an increased sensitivity to the drug in HEK293 cells stably overexpressing PKM2 ($\sim$2-fold estimated by Western blot; Fig. 1*D*). Unfortunately, small interfering RNA treatment against PKM2 was inefficient; therefore, we were not able to test the effect of downregulation of the protein on TT-232 sensitivity.

Translocation of PKM2 into the nucleus. Using surface plasmon resonance, we found that TT-232 interferes with the interaction of PKM2 and tubulin without influencing its enzymatic activity (data not shown). Encouraged by the observation of TT-232–induced PKM2 dissociation from microtubules, we investigated the subcellular localization of PKM2 on TT-232 stimulation. PKM2 was found to translocate into the nucleus of TT-232–treated Cos-7 cells both by PKM2 immunostaining with a polyclonal antibody (Fig. 2*A*) and using PKM2 that was NH_2-terminally fused to GFP protein (Fig. 2*B* and *C*). To further analyze the nuclear translocation of PKM2, we separated TT-232–treated Cos-7 cells into cytosolic, membrane, and nuclear fractions and analyzed these by immunoblotting with a PKM2 antibody. Endogenous PKM2 appeared in the nuclear extracts of TT-232–treated Cos-7 cells after 2 h treatment with the drug. In these experiments, to exclude cross-contamination, samples were immunoblotted with antibodies to Erk-2 or histone H1 in addition to PKM2 (Fig. 2*D*) Nuclear PKM2 displayed increased mobility in

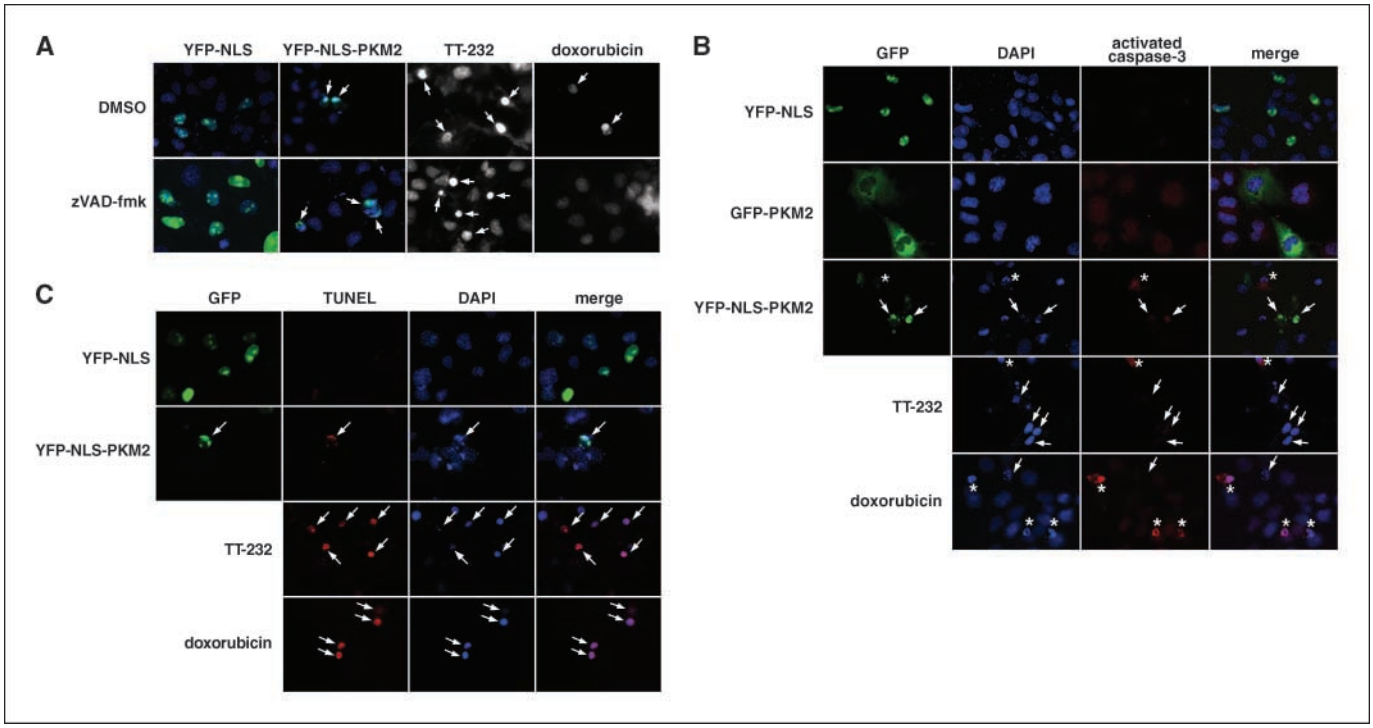

Figure 5. Nuclear PKM2 and TT-232 induce a caspase-independent apoptosis. *A,* Cos-7 cells were transfected with EYFP fused to the SV40 large T antigen NLS (*YFP-NLS*) or with pEYFP-NLS-PKM2 (*YFP-NLS-PKM2*) and treated with DMSO or zVAD-FMK in DMSO. Alternatively, cells were pretreated with DMSO or zVAD-FMK, and cell death was induced with 50 μmol/L TT-232 or 10 μmol/L doxorubicin. Highly fluorescent, condensed, fragmented nuclei were considered as being apoptotic (*arrows*). *B,* Cos-7 cells were transfected with EYFP fused to the SV40 large T antigen NLS (*YFP-NLS*), pEGFP-PKM2 (*GFP-PKM2*), and pEYFP-NLS-PKM2 (*YFP-NLS-PKM2*) or treated with 50 μmol/L TT-232 or 10 μmol/L doxorubicin for 24 h. Cells were fixed and immunostained with activated caspase-3 antibody. *Arrows,* apoptotic cells; *, activated caspase-positive cells. *C,* Cos-7 cells were transfected with EYFP fused to the SV40 large T antigen NLS (*YFP-NLS*) and with pEYFP-NLS-PKM2 (*YFP-NLS-PKM2*) or treated with 50 μmol/L TT-232 or 10 μmol/L doxorubicin for 24 h. Cells were fixed and TUNEL staining was done. *Arrows,* TUNEL-positive cells.

SDS gels, possibly reflecting proteolytic cleavage or dephosphorylation. Because pretreatment with inhibitors of serine-proteases (AEBSF and TPCK), caspases (zDEVD), or calpain (ALLN) did not revert this effect (data not shown), the mechanism of PKM2 processing and its significance during nuclear translocation remain to be elucidated.

We next showed that besides TT-232, 100 μmol/L hydrogen peroxide (H_2O_2) or 120 mJ/cm^2 UV light also induced nuclear translocation of PKM2 preceding the appearance of nuclear apoptotic morphology (Fig. 3*A*). To confirm this result, untransfected Cos-7 cells were treated with H_2O_2 or UV light, separated into cytosolic and nuclear fractions, and analyzed by immunoblotting with PKM2 antibody (Fig. 3*B* and *C*). Indeed, PKM2 was found in the nuclear fractions of H_2O_2- or UV-treated Cos-7 cells with a similar kinetics as observed for TT-232 somatostatin analogue. Furthermore, both peroxide and UV increased the mobility of nuclear PK, which suggests the activation of a similar mechanism in response to all three treatments. Taken together, these results supported our hypothesis that PKM2 translocates into the nucleus in response to different apoptotic stimuli.

Because PKM2 is predominantly expressed in tumor cells (18–20), we wanted to know whether nuclear translocation is sufficient to induce apoptosis and if this effect is isoform specific. To address this question, we fused PKM2 and PKM1 isoforms to GFP or SV40 large T-antigen nuclear localization signal (NLS)–tagged YFP and used YFP protein alone as a control. Indeed, using the 3-(4,5-dimethylthiazol-2-yl)-2,5-diphenyltetrazolium bromide (MTT) assay, we observed significant growth inhibition of cells that were transfected with the nuclear-targeted NLS-PKM2, whereas proliferation of Cos-7 cells expressing GFP, YFP-NLS, or PKM2 was unaffected (Fig. 4*A*). In contrast, nuclear targeting of PKM1 (YFP-NLS-PKM1) did not inhibit cell growth (Fig. 4*B*). To investigate this differential effect of the isoforms further, we analyzed transfected Cos-7 cells on staining with Hoechst 33258 under fluorescent microscope. YFP-NLS-PKM2 was found in the nucleus and cells expressing this protein construct showed highly fluorescent, condensed, fragmented nuclei that formed patches of compact chromatin and hence were identified as apoptotic cells (Fig. 4*C*). In contrast, GFP-PKM2 was cytoplasmic, and cells expressing the fusion protein showed normal nuclear staining similar to cells expressing GFP or YFP-NLS. At the same time, nuclear targeting of PKM1 had no detectable effect (Fig. 4*C*). We tested the role of caspases in TT-232– or PKM2-induced apoptosis in detail. First, we preincubated Cos-7 cells with zVAD-FMK, pan-caspase inhibitor that efficiently blocked doxorubicin-induced apoptosis, but had no effect on TT-232– or YFP-NLS-PKM2–induced cell death (Fig. 5*A*). Furthermore, activation of caspase-3 was observed only on doxorubicin treatment (Fig. 5*B*), whereas TT-232 or YFP-NLS-PKM2 resulted highly fluorescent, condensed, fragmented nuclei without dramatic change in the amount of activated caspase-3 (Fig. 5*B*). On the other hand, besides morphologic changes characteristic to apoptosis, YFP-NLS-PKM2– or TT-232–treated cells were positive for TUNEL staining (Fig. 5*C*), supporting the idea that both TT-232 and nuclear localization of PKM2 induce apoptosis that is independent of the classic caspase-mediated apoptotic machinery.

Finally, we studied the requirement of the enzymatic activity of nuclear PKM2 for the induction of apoptosis. We generated a kinase-deficient PKM2 mutant (K294M), transfected it into Cos-7 cells, and measured total PK activity as described previously (24). As shown in Fig. 6*A* and *B*, the expressed mutant protein interfered with the activity of the endogenous PKM2. This indicated that mutation of the critical Lys^{294} residue abolishes the catalytic activity of PKM2, likely via formation of mixed tetramers consisting of endogenous active and ectopically expressed inactive M2 subunits. Next, we overexpressed the nuclear-targeted kinase-deficient PKM2 in Cos-7 cells and we show that YFP-NLS-PKM2wt as well as YFP-NLS-PKM2 K294M were found in the nucleus, and cells expressing these proteins displayed an apoptotic morphology at a comparable level (Fig. 6*C*). Putting these results in relation with the fact that nuclear translocation of catalytically active PKM1 did not induce chromatin condensation (Fig. 4); we concluded that the catalytic activity of nuclear PKM2 is not required for the induction of apoptosis.

Discussion

We have shown that both somatostatin and the tumor-selective anticancer somatostatin analogue TT-232 interact with PKM isoform. The affinity of PKM toward the peptides is in the nanomolar range, although the cytosolic availability of the two peptides might be considerably different. Somatostatin or conventional somatostatin analogues interact with six different seven-pass transmembrane receptor on the cell surface. The ligand-receptor interaction is of high affinity; therefore, these peptides bind predominantly to the cell surface receptors and induce a multitude of signaling events before being sequestered and rapidly degraded (3). Although TT-232 could also interact with a subset of somatostatin receptors (mainly SSTR-1 and SSTR-4), its affinity is considerably lower (5). Nevertheless, TT-232 could activate signaling cascades mediated by these receptors while not being sequestered and degraded efficiently by the endocytic-lysosomic pathway. This allows the peptide to pass the cell membrane and accumulate in the cytosol. Indeed, we found previously that the uptake of TT-232 is crucial for the induction of apoptosis (4, 8).

TT-232, somatostatin, or other analogues interact with the cytosolic PK and consequently causes the PKM2 isoform to translocate into the nucleus. Such a translocation is also observed on treatment with reactive oxygen species–generating agents, such as H_2O_2 and UV radiation. Because oxidative stress (25) and UV (26) were found to disrupt microtubules, PKM2 could be released, suggesting a similar mechanism as found for TT-232. Previously, nuclear translocation of glyceraldehyde-3-phosphate dehydrogenase (GAPDH) on apoptotic stimulation of cells was reported (27–29). Furthermore, antisense oligonucleotide targeting of GAPDH partially prevents cell death (29). Other glycolytic enzymes, such as lactate dehydrogenase, phosphoglycerate kinase, and aldolase, also have been reported to display nuclear localization (30). In the current study, we show that nuclear translocation of PKM2 is sufficient and necessary for the induction of programmed cell death. These findings strongly suggest that changing the subcompartmental distribution of metabolic proteins (e.g., cytochrome *c* and GAPDH) is a general mechanism for the induction of cell death. Alternatively, glycolytic enzymes could cooperate in the nucleus to induce cell death.

For PKM, the induction of apoptosis is isoform specific and selective for the tumor marker PKM2 protein. This form of PK, a key regulator of cell metabolism, is widely used in tumor diagnostics (20). Our findings strongly suggest that it could also present a novel opportunity to selectively target tumor cells. Interestingly, the kinase activity of PKM2 is not required for the

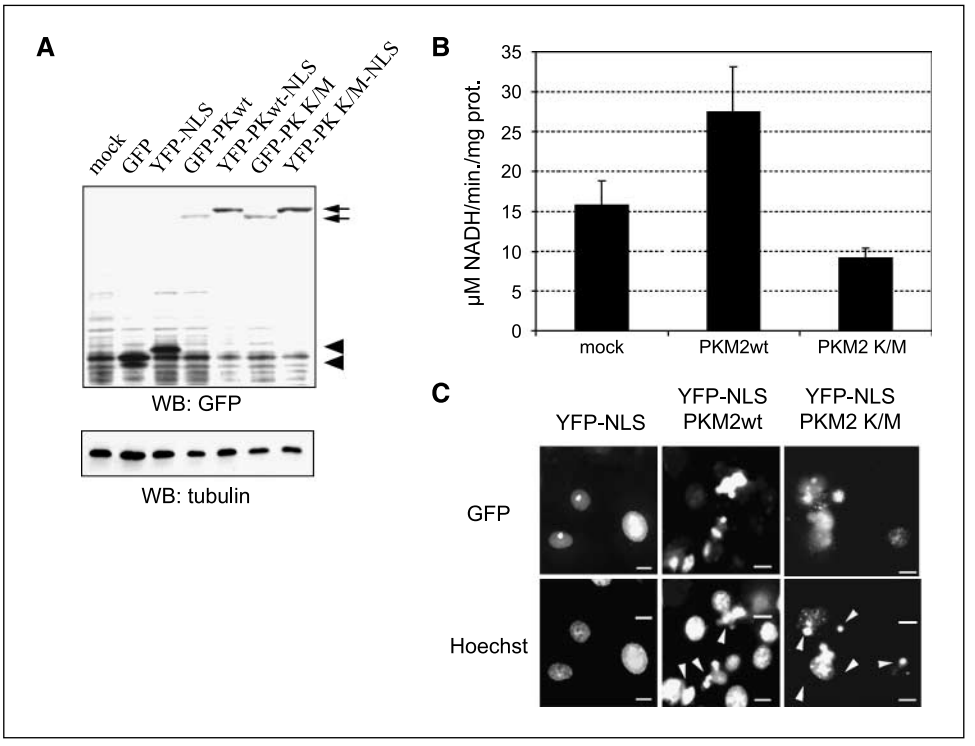

Figure 6. The activity of nuclear PKM2 is not required for the induction of apoptosis. *A,* Cos-7 cells were transfected with pEYFP-NLS (*YFP-NLS*), wild-type (WT) pEYFP-NLS-PKM2 (*YFP-NLS-PKM2*), or catalytically inactive pEYFP-NLS-PKM2 (*YFP-NLS PKM2 K/M*), and the expression and stability of the GFP fusion proteins were analyzed by Western blotting. Tubulin staining was used as a loading control. *Arrows*, GFP fusion proteins; *arrowheads*, GFP alone. *B,* Cos-7 cells were transfected with vector (*mock*), WT pEYFP-NLS-PKM2 (*PKM2wt*), or catalytically inactive pEYFP-NLS-PKM2 (*PKM2 K/M*), and the catalytic activity of PK was measured (n = 9 of three independent experiments). *Bars*, SD. *C,* Cos-7 cells were transfected with pEYFP-NLS (*YFP-NLS*), WT pEYFP-NLS-PKM2 (*YFP-NLS PKM2wt*), or catalytically inactive pEYFP-NLS-PKM2 (*YFP-NLS PKM2 K/M*) and incubated for 48 h in FCS-containing medium. Cells were fixed and analyzed under fluorescent microscope for GFP (*top*) and for nuclear staining (*bottom*). Highly fluorescent, condensed, fragmented nuclei were considered as being apoptotic (*arrowheads*). *Scalebar*, 50 μm.

induction of a caspase-independent cell death. It is therefore likely that nuclear translocation of PKM2 is not inducing cell death via depletion of cytosolic PKM2 tetramers that could cause a collapse of the energy metabolism of cells but is rather required for the formation of a nuclear cell death complex. This idea is further supported by the fact that overexpression of an inactive form of the enzyme decreases the overall metabolic rate of cells without triggering apoptosis.

In summary, our results show that the tumor-specific PKM2 is involved in a novel form of caspase- and Bcl-2–independent apoptosis and thereby shed new light on the function of PK in the cell. Whether the underlying mechanism is similar to that of apoptosis-inducing factor (31) remains to be elucidated. Our findings validate PKM2 as a promising, generally relevant target for the development of anticancer therapies with broad efficacy.

Acknowledgments

Received 8/2/2006; revised 10/31/2006; accepted 12/16/2006.

Grant support: OTKA/T049478, NKFP 1A/0020/2002, FP6-2003-LIFESCIHEALTH-I, and NKFP 1A005/2004 grants and the Max-Planck Society.

The costs of publication of this article were defrayed in part by the payment of page charges. This article must therefore be hereby marked *advertisement* in accordance with 18 U.S.C. Section 1734 solely to indicate this fact.

We thank G. Staal for PKM2 antibody and J. Kellermann for protein sequencing support.

References

1. Bertherat J, Bluet-Pajot MT, Epelbaum J. Neuroendocrine regulation of growth hormone. Eur J Endocrinol 1995;132:12–24.

2. Patel YC. Somatostatin and its receptor family. Front Neuroendocrinol 1999;20:348–67.

3. Lahlou H, Guillermet J, Hortala M, et al. Molecular signaling of somatostatin receptors. Ann N Y Acad Sci 2004;1014:121–31.

4. Kéri G, Erchegyi J, Horvath A, et al. A selective-selective somatostatin analog (TT-232) with strong *in vitro* and *in vivo* antitumour activity. Proc Natl Acad Sci U S A 1996;93:12513–8.

5. Stetak A, Lankenau A, Vantus T, Csermely P, Ullrich A, Keri G. The antitumor somatostatin analogue TT-232 induces cell cycle arrest through PKCδ and c-Src. Biochem Biophys Res Commun 2001;285:483–8.

6. Stetak A, Csermely P, Ullrich A, Keri G. Physical and functional interactions between protein tyrosine phosphatase α, PI 3-kinase, and PKCδ. Biochem Biophys Res Commun 2001;288:562–72.

7. Diaconu CC, Szathmari M, Keri G, Venetianer A. Apoptosis is induced in both drug-sensitive and multidrug-resistant hepatoma cells by somatostatin analogue TT-232. Br J Cancer 1999;80:1197–203.

8. Vantus T, Kéri G, Krivickiene Z, et al. The somatostatin analogue TT-232 induces apoptosis in A431 cells: sustained activation of stress-activated kinases and inhibition of signalling to extracellular signal-regulated kinases. Cell Signal 2001;13:717–25.

9. Kéri G, Mezö I, Horvath A, et al. Novel somatostatin analogues with tyrosine kinase inhibitory and antitumour activity. Biochem Biophys Res Commun 1993;191:681–7.

10. Kéri G, Mezö I, Vadasz Z, et al. Structure-activity relationship studies of novel somatostatin analogs with antitumour activity. J Pept Res 1993;6:281–8.

11. Tanaka T, Harano Y, Sue F, Morimura H. Crystallization, characterization, and metabolic regulation of two types of pyruvate kinase isolated from rat tissues. J Biochem (Tokyo) 1967;62:71–91.

12. Nowak T, Suelter C. Pyruvate kinase: activation by and catalytic role of the monovalent and divalent cations. Mol Cell Biochem 1981;35:65–75.

13. Ibsen K, Trippet P. Effects of amino acids on the kinetic properties of three noninterconvertible rat pyruvate kinases. Arch Biochem Biophys 1974;163:570–80.

14. Kato H, Fukuda T, Parkinson C, McPhie P, Cheng SY. Cytosolic thyroid hormone-binding protein is a monomer of pyruvate kinase. Proc Natl Acad Sci U S A 1989;86:7861–5.

15. Vértessy BG, Bankfalvi D, Kovacs J, Low P, Lehotzky A, Ovadi J. Pyruvate kinase as a microtubule destabilizing factor *in vivo*. Biochem Biophys Res Commun 1999;254:430–5.

16. Dabrowska A, Pietkiewicz J, Dabrowska K, Czapinska E, Danielewicz R. Interaction of M1 and M2 isozymes pyruvate kinase from human tissues with phospholipids. Biochim Biophys Acta 1998;1383:123–9.

17. Takenaka M, Yamada K, Lu T, Kang R, Tanaka T, Noguchi T. Alternative splicing of the pyruvate kinase M gene in a minigene system. Eur J Biochem 1996;235:366–71.

18. Mellati A, Yucel M, Altinors N, Gunduz U. Regulation of M2-type pyruvate kinase from human meningioma by allosteric effectors fructose 1,6 diphosphate and L-alanine. Cancer Biochem Biophys 1992;13:33–41.

19. Guminska M, Stachurska MB, Ignacak J. Pyruvate kinase isoenzymes in chromatin extracts of Ehrlich ascites tumour, Morris hepatoma 7777, and normal mouse and rat livers. Biochim Biophys Acta 1988;966:207–13.

20. Oremek GM, Teigelkamp S, Kramer W, Eigenbrodt E, Usadel K-H. The pyruvate kinase isoenzyme tumor M2 (Tu M2-PK) as tumor marker for renal carcinoma. Anticancer Res 1999;19:1599–602.

21. Presek P, Reinacher M, Eigenbrodt E. Pyruvate kinase type M2 is phosphorylated at tyrosine residues in cells transformed by Rous sarcoma virus. FEBS Lett 1988;242:194–8.

22. Partis MD, Griffiths DG, Roberts GC, Beechey RB. Cross-linking proteins by ω-maleimido alkanoyl n-hydroxysuccinimido esters. J Protein Chem 1983;2:263–77.

23. Weernink PAO, Rijksen G, Staal GEJ. Production of a specific antibody against pyruvate kinase type M2 using a synthetic peptide. FEBS Lett 1988;236:391–5.

24. Leong SF, Lai JCK, Lim L, Clark JB. Energy-metabolising enzymes in brain regions of adult and aging rats. J Neurochem 1981;37:1548–56.

25. Valen G, Sondén A, Vaage J, Malm E, Kjellström BT. Hydrogen peroxide induces endothelial cell atypia and cytoskeleton depolymerization. Free Radic Biol Med 1999;26:1480–8.

26. Zamansky GB, Perrino BA, Chou I. Disruption of cytoplasmic microtubules by ultraviolet radiation. Exp Cell Res 1991;195:269–73.

27. Dastoor Z, Dreyer J. Potential role of nuclear translocation of glyceraldehyde-3-phosphate dehydrogenase in apoptosis and oxidative stress. J Cell Sci 2001;114:1643–53.

28. Shashidharan P, Chalmers-Redman RM, Carlile GW, et al. Nuclear translocation of GAPDH-GFP fusion protein during apoptosis. Neuroreport 1999;10:1149–53.

29. Shawa A, Khan AA, Hester LD, Snyder SH. Glyceraldehyde-3-phosphate dehydrogenase: nuclear translocation participates in neuronal and nonneuronal cell death. Proc Natl Acad Sci U S A 1997;94:11669–74.

30. Ronai Z. Glycolytic enzymes as DNA binding proteins. Int J Biochem 1993;25:1073–6.

31. Susin SA, Lorenzo HK, Zamzami N, et al. Molecular characterization of mitochondrial apoptosis-inducing factor. Nature 1999;397:441–6.